

# Mechanisms of Pinning Accompanying Evaporation of Colloidal Dispersion Droplets

S. P. Molchanov<sup>a, b</sup>, V. I. Roldugin<sup>c, \*</sup>, I. A. Chernova-Kharaeva<sup>b</sup>, and G. A. Yurasik<sup>b</sup>

<sup>a</sup>Topchiev Institute of Petrochemical Synthesis, Russian Academy of Sciences, Leninskii pr. 29, Moscow, 119071 Russia

<sup>b</sup>Photochemistry Center, Russian Academy of Sciences, ul. Novatorov 7a, bldg. 1, Moscow, 119421 Russia

<sup>c</sup>Frumkin Institute of Physical Chemistry and Electrochemistry, Russian Academy of Sciences, Leninskii pr. 31, bldg. 4, Moscow, 119071 Russia

\*e-mail: vroidugin@yandex.ru

Received September 7, 2016

**Abstract**—Experiments have been performed to clarify the mechanism of pinning, i.e., the phenomenon of fixing menisci of evaporating dispersion droplets, related to the formation of ring-shaped deposits (coffee ring effect). The influence of particle concentration in dispersions and the degree of hydrophilicity (hydrophobicity) of substrates on pinning has been studied. It has been shown that there are three main mechanisms of pinning, with the first one being due to the hysteresis of droplet contact angle, the second mechanism resulting from the adhesion of particles to substrates, and the third one being caused by the formation of a dense adsorption layer on a substrate. A relation has been revealed between the pinning mechanism that occurs and the degree of substrate hydrophilicity.

DOI: 10.1134/S1061933X17020089

## 1. INTRODUCTION

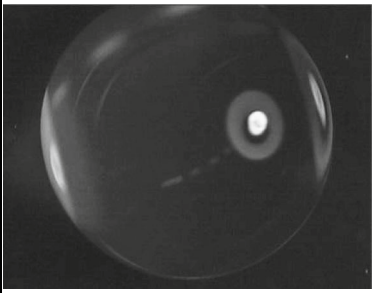
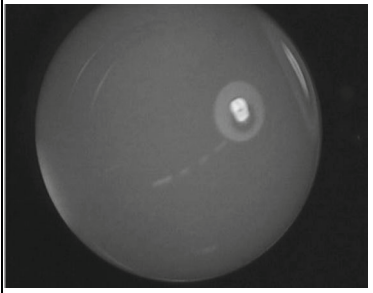
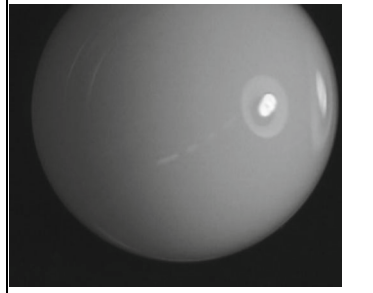
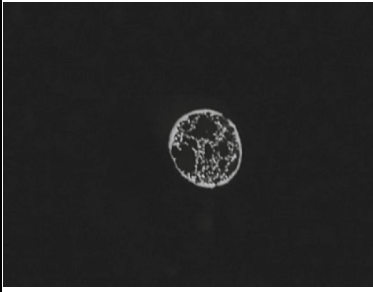
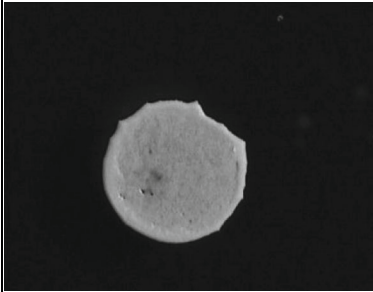
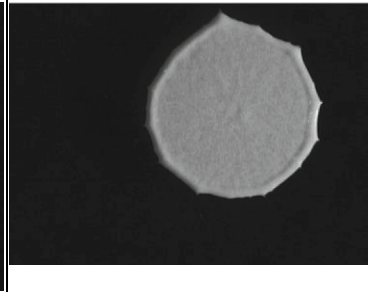
In [1–3], we began to study systematically the regularities of the formation of ring-shaped deposits upon the evaporation of dispersion droplets. This phenomenon, which was, for the first time, considered in [4, 5] and called the “coffee-ring effect” (CRE), has attracted the attention of many researchers. Subsequent experiments have shown that the processes accompanying droplet evaporation have a rather complex character and are governed by both the individual and collective behaviors of colloidal particles. The mechanism that leads to the formation of ring-shaped deposits with the observed diversity of the structures remains to be studied. However, this circumstance does not prevent the CRE from being used in practice [6, 7].

In addition to the aforementioned individual/collective behavior of particles, the difficulties that are encountered when clarifying the fine peculiarities of the ring-shaped deposits originate from the simultaneous action of different factors, namely, the properties of a dispersion medium [8]; the state of the particle surface, which predetermines the interparticle interaction [8]; and the shapes and sizes of the particles [10, 11]. An important role is also played by the composition of a dispersion medium, especially the presence of surfactants in it [12]. The influence of a substrate has also appeared to be rather strong [1–3, 13–18]. In addition to the expected important role of the hydro-

philicity (hydrophobicity) of a substrate in the formation of a deposit structure, the thermophysical characteristics of a substrate have unexpectedly appeared to be of significance [19, 20]. This experimental fact suggests that the structure of a deposit being formed must be strongly affected by the dynamics of droplet evaporation. The important role of dynamic processes in the formation of self-organized ensembles of colloidal particles has also been observed in other situations [21–25].

This work continues our previous studies [1–3]. Among our earlier results, three main scenarios established for the formation of ring-shaped deposits should be distinguished [2]. These scenarios have been conventionally classified as follows: “droplet evaporation from the center to the periphery with the formation of a ring-shaped deposit,” “droplet evaporation from the periphery to the center with the formation of a ring-shaped deposit,” and “droplet evaporation from the periphery to the center with the formation of a disk-shaped deposit” and imply the following droplet evaporation regimes: “at an unchanged radius,” “at an unchanged shape,” and a combined regime “at both radius and shape being changed.” Note that the possibility of realization of only two main scenarios of droplet evaporation under the conditions of CRE was previously noted in the literature [26]. It was also shown [3] that, under certain conditions, droplet evaporation scenarios may replace each other, with the

Comparative characteristics of deposits resulting from evaporating droplets of DPSPs with different concentrations and corresponding photographs

DPSP concentration, wt %	0.01	0.25	1
Droplet photograph			
Deposit photograph			
Relative pinning radius	0.25	0.46	0.62

replacement being associated with the main phenomena that accompany the development of CRE. This concerns the phenomena of pinning (a fixed position of the meniscus of an evaporating dispersion droplet) and depinning (meniscus movement after some period of its quiescence). That is, it may be stated that pinning and depinning predetermine the structure of a resulting deposit. In this work, we shall consider the mechanisms responsible for pinning; depinning will be discussed in a subsequent communication.

## 2. MATERIALS AND METHODS

Experiments were performed with droplets of dispersions of polystyrene latex particles (DPSP-1) with diameters  $d = 210 \pm 60$ ,  $250 \pm 60$ , and  $540 \pm 60$  nm [28] and dispersions of silica particles (DSPs) with  $d = 230 \pm 10$  nm obtained by tetraethoxysilane hydrolysis in ethanol in the presence of ammonia as a catalyst [29]. Polystyrene particles contained surface  $\text{NH}^-$  and  $\text{COO}^-$  groups in a concentration of  $2 \times 10^{-6}$  mol/m<sup>2</sup>. In addition, dispersions of polystyrene latex particles (DPSP-2) with a size of  $540 \pm 30$  nm (PolymerLatex GmbH & Co, Germany) were used.

Particle sizes were determined by dynamic light scattering with a Photocor Complex spectrometer (Fotocor Ltd, Russia).

Particles were dispersed in deionized water obtained by sorption and ion-exchange filtration followed by mechanical microfiltration in a D-301 deionizer (Akvilon, Russia). The same deionized water was used in experiments with the particle-free dispersion medium.

LOT 18414 219 microscope slides (MSs) (Marienfeld, Germany) with sizes of  $76 \times 26 \times 1$  mm<sup>3</sup> preliminarily cleaned from contaminants were used as hydrophilic substrates.

The MS surface was treated as follows. Initially, an MS was mechanically cleaned with cotton wetted with 2-propanol and, then, with dry cotton. After that, the MS was treated with an air jet.

MSs coated with a polystyrene film (500 nm thick) on a Spincoater P6700 setup (Specialty Coating Systems, United States) were used as hydrophobic substrates. The films were formed in the following way. Initially, a saturated polystyrene solution in toluene was prepared. For this purpose, polystyrene (0.1 g) and toluene (0.8 mL) were placed into an Eppendorf tube, which was exposed in a thermoshaker for 60 min (1400 rpm, 50°C). Then, the polymer solution (100  $\mu\text{L}$ ) was applied onto cleaned MSs with a Spincoater P6700 setup at 2000 rpm for 1 min. Computer disks, the working surface of which had a protective layer of a fluoroorganic polymer, were also used as hydrophobic substrates.

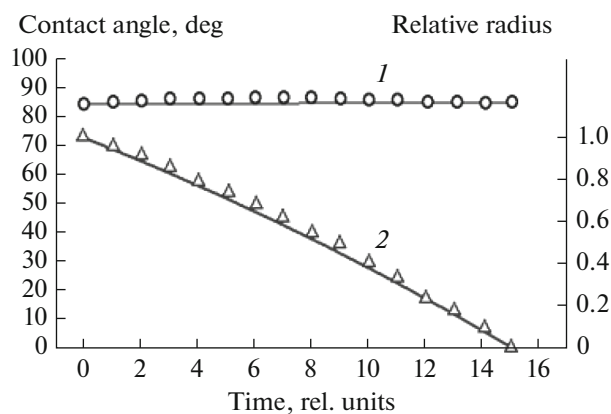


**Fig. 1.** Time dependences of the (1) contact angle and (2) relative radius of a deionized water droplet on a hydrophobic polystyrene substrate; an interval of 200 s corresponds to unit time.

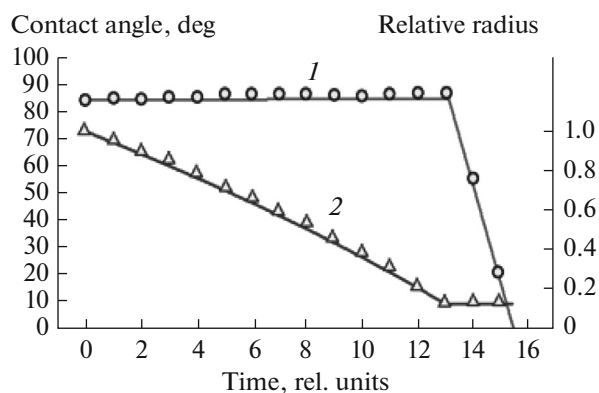


**Fig. 2.** Time dependences of the (1) contact angle and (2) relative radius of a deionized water droplet on a hydrophobic substrate made of a computer disk; an interval of 150 s corresponds to unit time.

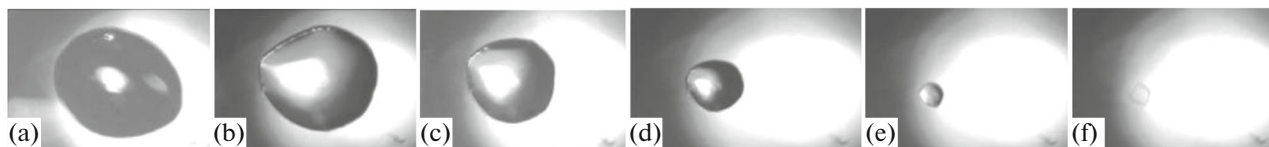


**Fig. 3.** Photographs taken from a 20- $\mu$ L deionized water droplet after evaporation for (a) 0, (b) 24, (c) 31, (d) 37, (e) 40, and (f) 41 min.

Experiments were also carried out with polymer films of different compositions, the surfaces of which were modified by different methods (see [3]) to vary the contact angle in a wide range of its values.

Before the experiments on droplet evaporation, the dispersions were treated in a UZV-2 ultrasonic bath (Sapfir, Russia) for 15 min.

Microdroplets were applied onto a substrate using a manual Lempipet Digital dosing pipette equipped with replaceable heads, which enabled us to obtain droplets with sizes of 2–40  $\mu$ L.

Droplets with picosized volumes were applied using a Jetlab II setup (MicroFab Inc., United States). The generated microdroplets had the following parameters: velocity at the nozzle outlet of  $2.3 \pm 0.2$  m/s, volume of  $230 \pm 25$  pL, diameter of  $78 \pm 2$   $\mu$ m, and angle of deviation from the vertical of no more than  $1^\circ$ .

The droplets were monitored using the video camera supplied with the Jetlab II setup and a SolverBio scanning probe microscope (SPM) (NT-MDT, Russia). The contact angles were measured with the help of an optical video stand (Photochemistry Center, Russian Academy of Sciences) [24] consisting of a measuring table for a substrate onto which a droplet was applied, as well as vertical and horizontal long-focus microscopes equipped with video cameras,

which monitored the droplet at different angles. Before a droplet was applied, a substrate was placed onto the measuring table; then, the droplet images were begun to be recorded (the top and side views) with preset time intervals. After that, a droplet of a specified volume was applied onto the substrate. The droplet images were taken until it was completely evaporated. The obtained images were used to determine all necessary parameters, i.e., the initial and current contact angles, pinning angle, sizes of the droplet contact spot and the solid deposit, the pinning radius and its duration, etc. Special software was used to determine accurately the contact angle of a droplet from the parameters of its side-view image (Photochemistry Center, Russian Academy of Sciences, Russia).

The experiments were carried out under standard laboratory conditions: the temperature of the solutions, substrates, and environment was  $20^\circ\text{C}$ , and the relative humidity was 25%.

### 3. PINNING

As has been noted in the Introduction, the phenomenon of pinning, which consists in meniscus fixation on a substrate during the evaporation of a sessile droplet, is of fundamental importance for explaining the mechanism of CRE and the formation of resulting

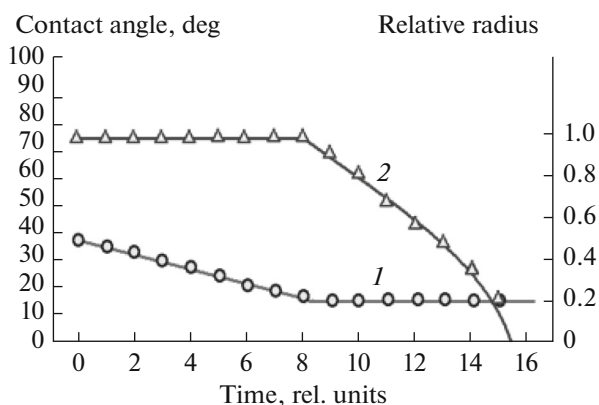


**Fig. 4.** Time dependences of the (1) contact angle and (2) relative radius of a deionized water droplet on a hydrophilic glass substrate; an interval of 180 s corresponds to unit time.

structures. This phenomenon is characterized by three main parameters, namely, pinning time (the time elapsed from the droplet application to the fixation (fastening) of its meniscus), pinning angle, and pinning diameter (the values of the contact angle and the base diameter of a droplet at the moment of meniscus fixation).

In this work, we shall consider the effects of substrate characteristics, the initial contact angle of a droplet, its volume, and the concentration and nature of particles in a colloidal dispersion on pinning. We shall illustrate the relation between the pinning parameters and the structures of deposits resulting from droplet evaporation and propose an original classification of its mechanisms. The matter is that the meniscus fixation may result from different causes, with only some of them being relevant to the CRE.

### 3.1. Pinning of the Meniscus of a Dispersion Medium Droplet

In some cases, droplet evaporation is not accompanied by pinning. The time dependences of the contact angle and the relative radius of a contact spot for a 10- $\mu$ L deionized water droplet on a glass substrate coated with a polystyrene film serve as an example (Fig. 1).

The dependences presented in Fig. 1 show that the droplet evaporates at a constant contact angle, with its radius gradually decreasing (regime “at an unchanged shape”). This process may be referred to as an “ideal” one, because, according to [2], even when a pure solvent is evaporated, the meniscus of an evaporating droplet may remain quiescent for some time; i.e., pinning is possible. Two variants may take place in this situation.

**3.1.1. Impurities and pinning.** One of the reasons for the appearance of pinning for a droplet of a for-

mally pure solvent is associated with the presence of impurities in it. The impurities may be both primordially present in a solvent and transferred into the bulk droplet from a substrate surface after the droplet application. Moreover, their concentration increases as the droplet evaporates.

This situation is illustrated in Fig. 2, which presents the time dependences of the contact angle and relative radius of a 20- $\mu$ L droplet of deionized water evaporating on a substrate made of a computer disk. Time variations in the size and shape of the droplet are shown in Fig. 3. A ring-shaped deposit that has remained on the surface after droplet evaporation indicates the presence of impurities in water. It is obvious that, in this case, the droplet volume plays a significant role; the larger the volume, the larger the amount of impurities that will remain in the final deposit and affect the moment of pinning onset.

The aforementioned figures show that the droplet initially evaporates in the regime “at an unchanged shape.” However, at a certain stage, its meniscus is fixed (pinning takes place); later, the droplet evaporates with the quiescent meniscus in the regime “at an unchanged radius,” leaving a faint trace.

Thus, the presented data indicate that two evaporation regimes may be realized for droplets of “pure” solvents on hydrophobic substrates depending on the purity of a solvent–substrate system: (1) in the case of an “ideally” pure system, the droplet evaporates at a constant contact angle, while its radius gradually varies, and (2) in the presence of impurities, the initial stage resembles the “ideal” regime; however, at the final stage, the pinning of the meniscus takes place, which “switches over” the evaporation regime. It may be concluded that the appearance of pinning at the final stage of droplet evaporation indicates the presence of impurities in the droplet substance, while the pinning time characterizes their amount.

**3.1.2. Wetting hysteresis and pinning.** A somewhat different situation arises on a hydrophilic substrate. Experiments on droplet evaporation on hydrophilic substrates [2] have shown that, initially, the droplet meniscus may remain quiescent for a long time; i.e., pinning takes place from the very beginning. In this case, pinning is associated with the hysteresis of the contact angle [27]. Being applied onto a substrate, droplets fly down onto it at some velocity, so we may consider them as “advancing” on the surface. The advancing contact angle is larger than the receding angle. Therefore, the initial steady equilibrium contact angle appears to be larger than the receding angle, which determines the condition of meniscus movement along the substrate. Figure 4 presents the time dependences of the contact angle and contact-spot radius for a 10- $\mu$ L deionized water droplet on a glass substrate. It can be seen that, in contrast to the hydrophobic substrate, the initial stage of droplet evaporation occurs in the regime “at an unchanged radius”;

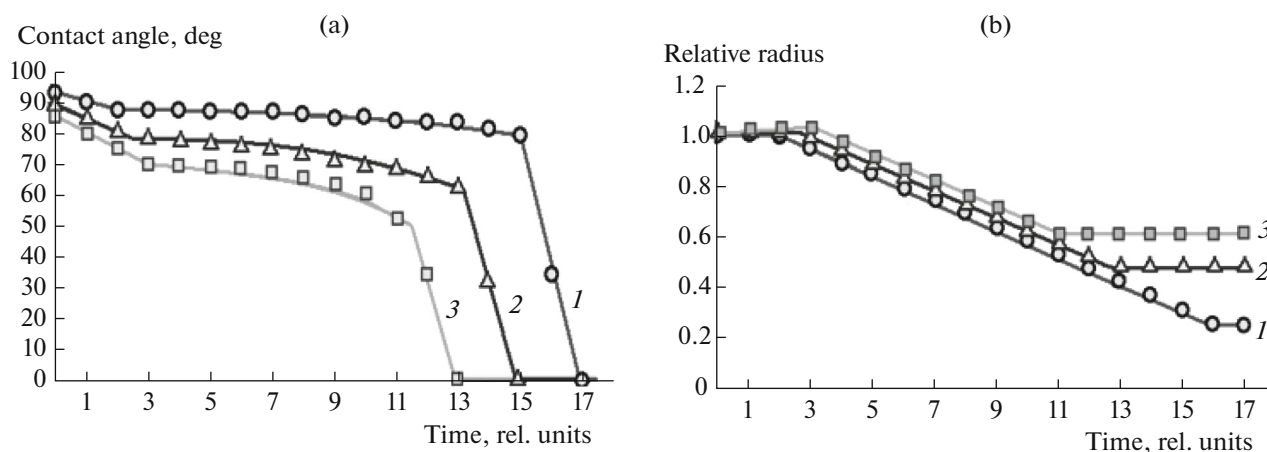


**Fig. 5.** Dependences of the current (a) contact angle and (b) relative radius on evaporation time for droplets of dispersions with concentrations of (1) 0.01, (2) 0.25 and (3) 1 wt %; an interval of 3 min corresponds to unit time.

i.e., the contact-spot radius remains unchanged, while the contact angle gradually decreases. When the contact angle becomes smaller than the receding one ( $15^\circ$ ), meniscus movement (depinning) begins. Therewith, the contact angle remains unchanged (equal to the receding angle), while the radius of the contact spot gradually decreases.

It is clear that, in the case of hydrophilic substrates, the occurrence and duration of pinning are mainly determined by the substrate characteristics, which affect the hysteresis of the contact angle.

### 3.2. Pinning of Dispersion Droplet Meniscus

As has been shown in [1–3], the “visiting card” of CRE is pinning, which, in most cases, takes place immediately after the application of a droplet onto a substrate. Pinning predetermines the development of ring-shaped deposit formation via the three scenarios [2] and, in the long run, the structure of a deposit. Hence, the main parameters affecting pinning and methods for the control over it must be searched for.

**3.2.1. Pinning and particle concentration in a solution.** As follows from all of the aforementioned, the presence of dispersed phase particles must, obviously, affect the pinning characteristics, at least, because they may be considered as an “impurity.” In this situation, particle concentration is, of course, the key factor. To clarify its role, experiments were preliminarily performed with droplets of dispersions, the concentrations of which were substantially different, while being rather low (see below). This enabled us to realize a situation in which pinning occurred not immediately after droplet application, but rather somewhat later, and was not accompanied by the rapid filling of the entire droplet contact spot with particles.

The experiments were performed with 5- $\mu\text{L}$  droplets of DPSP-2 samples having concentrations of 0.01, 0.25, and 1 wt %, which were applied onto a glass sub-

strate coated with a polystyrene film (the contact angle for water droplets of the same size was  $94^\circ$ ). Figure 5 shows the time dependences of the contact angle and relative radius of the droplet contact spot for the aforementioned dispersions.

Curves 1 in Figs. 5a and 5b indicate that the time dependences of the contact angle and radius for a droplet of the low-concentrated dispersion (0.01 wt %) almost coincide with those obtained for pure water (Figs. 1, 2). There are, however, the two following exceptions: (1) at the final stage of evaporation, pinning is observed, which is quite to be expected taking into account that the particles play the role of an impurity, which finally remains on the substrate, and (2) pinning is also observed at the initial stage, when it is due to the contact angle hysteresis. For a droplet of the dispersion with a concentration of 0.01 wt %, the contact angle decreases from an initial value of  $93^\circ$  to  $87^\circ$ ; then, it remains almost unchanged, while the meniscus moves until the onset of the final pinning, during which its value decreases from  $80^\circ$  to  $0^\circ$ . Note that, in contrast to a pure water droplet, the contact angle for the droplet of the low-concentrated dispersion is not constant, but rather decreases gradually.

As the dispersion concentration increases, the aforementioned influence of particles is enhanced. At a concentration of 0.25 wt %, the dependences deviate still greater from those observed for pure water; i.e., the critical receding angle and pinning angles have decreased, while the range of variations in the contact angle during meniscus movement and the radius of the contact spot at which the final spinning takes place have enlarged.

Greater deviations from the dynamics of pure water droplets are observed for a 1 wt % dispersion droplet, as can be distinctly seen from curves 3 in Fig. 5. Moreover, the contact-spot radius has even somewhat enlarged at an initial stage, and this finding may unambiguously be related to the increased concentra-

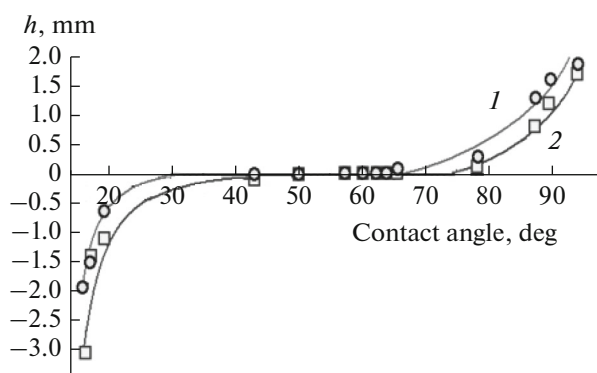


Fig. 6. Dependences of meniscus displacement  $h$  of (1) DPSP-1 and (2) DSP droplets on the contact angle.

tion of particles and their influence on the contact angle.

The comparative data on the three considered systems are presented in the table.

The image taken from the solid deposit upon the evaporation of a 0.01 wt % dispersion droplet distinctly shows a peripheral ring and an unfilled substrate regions inside it. Other images presented in the table indicate that some particles are fixed on the substrate before the three-phase contact line ceases to move. Hence, neither wetting hysteresis nor the formation of a densely packed layer of particles on the surface can be the reasons for the pinning in this case, while the cessation of meniscus movement is caused by the adhesion of the particles to the substrate at the three-phase contact line. This adhesion takes place upon increasing particle concentration (the analysis of the sizes of the ring-shaped deposits depicted in the table shows that, in the case of the dispersion with an initial concentration of 0.01%, the adhesion of the particles begins when their concentration has increased by no less than two orders of magnitude). As the meniscus moves, the particle concentration in the droplet increases, primarily at the three-phase contact line, thus leading to the formation of the ring-shaped deposit. Note that the deposits formed from dispersions with higher concentrations have the shape of a monolithic disk rather than that of a ring characteristic of the CRE. This suggests that the adhesion of the particles to the substrate occurs also in the internal region of the contact spot because of the relatively high concentration. Nevertheless, after the onset of pinning, the evaporation has occurred via the scenario “from the center to the periphery to yield a ring-shaped deposit” [2]. Obviously, this structure of the deposit results from the fact that, for a rather long period of time, the droplets evaporated in the regime “at an unchanged shape,” i.e., in the absence of compensatory flows transferring particles from the center to the periphery. In this situation, particles were uniformly accumulated at the liquid–gas interface, while the

total concentration of the dispersion grew. When the meniscus stopped moving (pinning began), the compensatory flows naturally arose; however, the droplet completely evaporated too soon for the formation of true peripheral rings. Therefore, only slight signs of the rings can be seen on the disks. Thus, it may be stated that, as the pinning time increases, the shape of a solid deposit varies from the ring-like to the disk-like one.

The aforementioned data show that, as the initial dispersion concentration increases, the value of the critical receding angle decreases. Moreover, the higher the initial particle concentration, the higher the rate of a reduction in the contact angle after the beginning of the meniscus movement; at the same time, the rate of decrease in the relative radius remains almost unchanged. Therewith, since the particle concentration in the droplet continuously increases, it may be concluded that the critical receding contact angle decreases. As the initial particle concentration increases, both the pinning contact angle and time decrease, while the deposit spot radius increases.

As we have shown in [1], the surface tension of a dispersion of polystyrene particles decreases with an increase in its concentration. This decrease may explain the reduction in the contact angle at which the meniscus begins to move. It also affects the pinning at the final stage of evaporation. A reduction in the surface tension decreases the force applied to the three-phase contact line in the direction toward the droplet center. Moreover, it may be assumed (here, special studies are required) that the adsorption of particles on a hydrophobic substrate (remember that air is considered to be a hydrophobic medium) also increases with particle concentration. A rise in the adsorption also enhances the probability of particle adhesion, after the onset of which the droplet evaporates with a fixed meniscus and a weak development of the compensatory flows, thereby leading to deposit formation via particle deposition, mainly in the form of a planar disk.

**3.2.2. Contact angle and pinning.** In this section, we shall consider the relation between the pinning and the initial contact angle. The experiments were performed with dispersions of two types; thus, we may, in some sense, take into account the effect the nature of particles. Evaporation of DPSP-1 and DSP droplets with particle diameters of 210 and 230 nm, respectively, was studied. Dispersion droplets with a volume of 20  $\mu\text{L}$  were applied onto polymer substrates treated in different ways (see [3] for details), thereby varying the contact angle from 16° to 94°. The value of meniscus displacement ( $h$ ) that occurs during the period from the moment of droplet application to the onset of pinning was recorded. Displacements of the meniscus toward the droplet center were considered to be positive. The pinning radius was determined as the radius of the

solid deposit. The results of the experiments are illustrated in Fig. 6.

The dependences presented in Fig. 6 show that, at small values of the initial contact angle, a droplet may spread until the onset of pinning. In this case, the diameter of the solid deposit is commonly larger than the initial contact spot diameter; i.e., displacement value  $h$  is negative. The value of  $h$  increases with a decrease in the contact angle; for DPSP-1, it is larger than for DSP.

At moderate values of the initial contact angle, the meniscus is fixed immediately at the moment of droplet application onto a substrate. In this case, the initial droplet diameter coincides with the solid deposit diameter. The mechanism of this effect will be considered in Section 4.

At large initial contact angles, pinning does not occur at once and is preceded by a decrease in the droplet size; it evaporates in the regime “at an unchanged shape” with the moving meniscus. The same case was considered in the previous section, however, without variations in the initial contact angle.

The observed different displacements of the three-phase contact line may be related to different adsorption values of particles at dispersion/air and dispersion/substrate interfaces and rate of their adhesion to the substrate. At a low rate of adhesion, particles have not time to essentially modify the surface, and, as a droplet evaporates, its meniscus moves toward the center. A rise in the concentration of particles at the meniscus as a result of droplet evaporation increases the probability of their adhesion, and, at some moment, the amount of the adhered particles becomes sufficient for meniscus fixation. This situation takes place at large contact angles. At small contact angles, movement in the opposite direction is possible, which may be related to the presence of a precursive film [30], from which particles may be deposited (see below), thus facilitating some spreading of the droplet.

**3.2.3. Pinning at high particle concentrations.** As has been mentioned above, when a dispersion droplet evaporates on a hydrophobic substrate, its meniscus is fixed after a substantial volume of water has evaporated from the droplet, and the three-phase contact line has been displaced toward the droplet center. Before this moment, the droplet evaporates in the regime “at an unchanged shape,” i.e., at a fixed contact angle (or its slow decreasing). In this case, the dispersed particles are “pushed” by the interfacial surface along the substrate surface toward the central region of the droplet. It has been shown that pinning takes place when some critical particle concentration is reached in the droplet. The pinning can be realized only when particles are fixed on the substrate at the three-phase contact line. A reduction in the surface tension of a colloidal solution also plays some role. However, in the case of hydrophobic substrates, the contact angle

may be close to  $90^\circ$ , thus noticeably enhancing the role of lateral components of the forces that displace the particles toward the droplet center and diminishing the role of their normal components that press the particles against the substrate. It is clear that, in this situation, the critical condition for the onset of pinning is determined by the degree of substrate surface coverage with the particles alone. It is reasonable to suppose that this critical degree of surface coverage is close to their dense packing. In this situation, the fixation of particles at the meniscus is predetermined by the dense packing of particles adsorbed on the substrate.

Let us consider the realization of this mechanism by the example of evaporating 280-pL microdroplets and 10- $\mu$ L macrodroplets ( $d = 540$  nm) of DPSPs with concentrations of 0.25, 0.5, 1, 2.5, 5, and 10 wt % on a hydrophobic substrate prepared as an MS coated with a polystyrene film (water contact angle is  $85^\circ$ ). The pinning radius was determined as the size of the deposit spot.

The experiments with the microdroplets were performed to study the packing of the particles in the deposit with the SPM and confirm that the packing is dense.

Figure 7 depicts an SPM image of a solid deposit resulted from evaporating a microdroplet of a 0.25 wt % dispersion. The deposit represents a hemisphere, which is formed by densely packed particles and reproduces the droplet shape. This witnesses that, at the pinning onset, the concentration of the particles in the droplet reaches a threshold value that corresponds to their dense packing. It is the establishment of the limiting packing that causes the stop of meniscus movement (pinning).

We failed to determine the profile of the deposit at a higher dispersion concentration, because the dynamic range of the SPM was exceeded. However, the conclusion that the deposits formed from droplets with different volumes and particle concentrations had similar shapes was inferred from the following considerations.

Figure 8 illustrates the dependences of relative pinning radius  $r/r_{0.25}$  on particle concentration, where the radius of a deposit formed from a droplet with a particle concentration of 0.25 wt % is used as the normalization value.

As can be seen from the figure, the patterns of the dependences plotted for the micro- and macrodroplets are almost identical, thus indicating the same mechanism of pinning and the similarity of the shapes of the deposits. The more rapid increase in the pinning diameter with the concentration for the macrodroplets (curve 2) suggests the more rapid passage to a deposit with a flattened shape. Deposit flattening with an increase in the particle concentration was established visually with an optical microscope. At the highest concentrations, deposits were even formed with slightly concave tops. The appearance of the concave

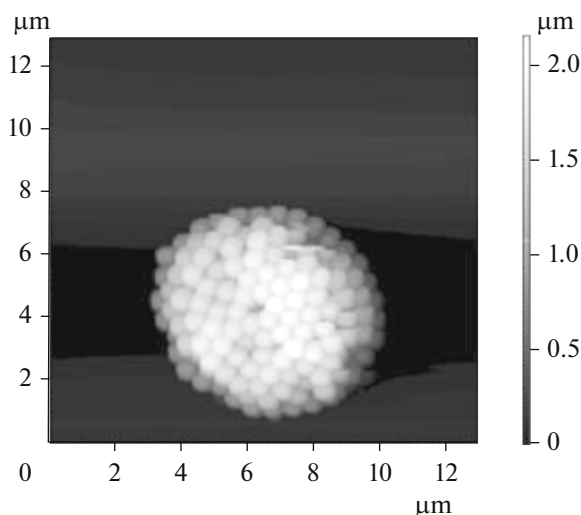


Fig. 7. SPM image of a deposit resulting from evaporating a DPSP-1 microdroplet on a polystyrene substrate.

regions is explained by the fact that the concentration of particles driven away by the interfacial surface is higher in the region of the meniscus, this leading to a larger height of the deposit at its periphery.

#### 4. RESULTS AND DISCUSSION

Let us use the aforementioned data to formulate a physical model of pinning taking into account only the compensatory flows and disregarding the Marangoni and Rayleigh flows.

After a droplet is applied onto a substrate, it acquires an equilibrium shape, which is governed by the balance of the capillary forces at the three-phase contact line. The value of the initial contact angle strongly affects the rate of droplet evaporation; i.e., the smaller the angle, the higher the evaporation rate (see [1–3] for details) and the velocity of the compensatory flows. Their velocity directly depends on the evaporation rate. Thus, the velocity of the compensatory flows is higher at small contact angles.

The contact angle also determines (indirectly) the character of the interaction between particles and a substrate. Since the particles are readily dispersed in water, their interaction (adsorption) must be more intense with a hydrophilic substrate than with a hydrophobic one. Thus, the pinning mechanism must primarily be determined by the initial contact angle. The pinning of a pure solvent is also governed by this angle, because the hysteresis of the contact angle is less pronounced (or absent) for a hydrophobic substrate.

Hence, when droplets evaporate on a hydrophobic substrate, their sizes decrease, with their shapes remaining self-similar; therefore, compensatory flows that would transfer the particles toward the meniscus are absent. The particles weakly interact with the sub-

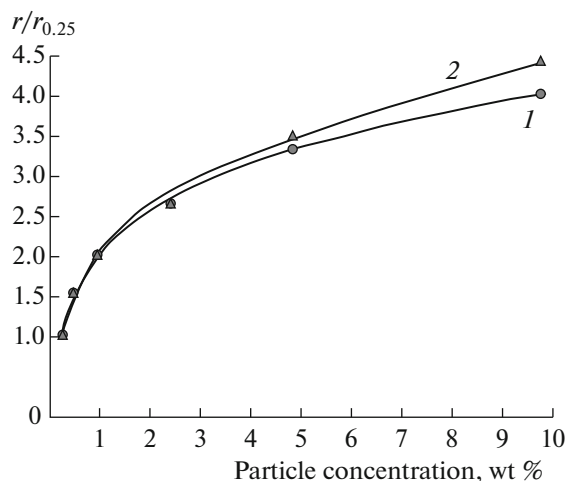


Fig. 8. Dependences of relative pinning radius for (1) microdroplets and (2) macrodroplets of dispersions on their initial concentrations.

strate surface and are displaced by the moving liquid/gas interface. A droplet evaporates in the regime “at an unchanged shape.” The adsorption of the particles on the substrate surface growth as their concentration increases. The surface tension of the dispersion somewhat varies, thereby affecting the contact angle of the moving meniscus. When a rather high particle concentration in the droplet is reached (owing to the evaporation of the dispersion medium), a densely packed layer of adsorbed particles is formed on the substrate. The moving meniscus “runs into” the adsorption layer, and pinning begins (Fig. 9). The further droplet evaporation leads to a decrease in the contact angle, which, at the onset of pinning, is markedly larger than the equilibrium one (the particles are “wetable” with water; therefore, the equilibrium contact angle is small on the layer of adsorbed particles). Evaporation in the regime “at an unchanged radius” begins. As the contact angle diminishes, compensatory flows develop and transfer the particles to the zone of the fixed meniscus. As a result, evaporation of



Fig. 9. The state of the adsorption layer of particles at the moment of meniscus fixation on a hydrophobic substrate.



rather large droplets results in the formation of droplets that have signs of a toroidal shape.

In the case of droplets on a hydrophilic substrate, the large difference between the advancing and receding contact angles results in the fact that, initially, pinning, which is also characteristic of the pure solvent, takes place. The smallness of the contact angle pre-determines the high intensity of the compensatory flows and the rapid transfer of particles to the meniscus. The intense interaction of the particles with the substrate results in their strong fixation. This may be, in particular, due to the following effect. In the case of hydrophilic substrates, a precursive film is rather rapidly formed in the region of the meniscus [30], with the concentration of dissolved substances dramatically increasing as this film evaporates. This promotes a reduction in the electrostatic potential barrier for the particles located near the substrate surface; therefore, they rapidly adhere to the surface. Note that our special studies have shown that particles in the meniscus are, indeed, so strongly bonded to a substrate that they are difficult to remove from it even under a strong mechanical action.

Since the particles are wettable with the dispersion medium, the equilibrium contact angle of water on their layer is small. Therefore, the meniscus “is anchored” to the particles adhered to the surface, and the droplet evaporates in the regime “at an unchanged radius” with a gradual decrease in the contact angle from the pinning angle to the equilibrium angle for the droplet on the layer of the particles (depinning angle). This is the main pinning mechanism for the majority of systems.

The additional transfer of particles to the region of the meniscus with the compensatory flows facilitates further reduction in the equilibrium contact angle, thus providing almost “absolute” fixation of the meniscus. The contact angle decreases until the thin water layer loses its stability (see [2]). We shall consider the behavior of the droplet after pinning in greater detail later when analyzing depinning.

Finally, a state of affairs is possible that is intermediate between those considered above and provides the realization of the main pinning mechanism in some period of time after the onset of droplet evaporation.

As has been mentioned above, the particle concentration increases while the meniscus moves. The concentration grows most rapidly at the liquid/vapor interface and, accordingly, at the liquid/substrate interface in the region of the meniscus. Here, the concentration of dissolved substances also increases, thus affecting the particle/substrate interaction. When some critical concentration is exceeded, the particles appear to be capable of overcoming the potential barrier of the interaction with the substrate and adhere to the latter. The fixation primarily occurs in the region of the meniscus, and the meniscus is, then, “anchored” to the fixed particles.

## 5. CONCLUSIONS

Thus, it has been shown that pinning, which is observed during droplet evaporation that is accompanied by the CRE, may have different physical causes. Three main mechanisms responsible for the pinning may be distinguished: the contact angle hysteresis, the formation of a dense layer of adsorbed particles, and their adhesion to a substrate. In the case of the formation of the dense layer, the adhesion of particles is not necessary for the onset of pinning. This mechanism is commonly realized for hydrophobic substrates. An increase in the substrate hydrophilicity facilitates the adhesion of particles due to a change in the character of their interaction with the substrate. A rise in the concentration of dissolved substances in the region of the meniscus and the precursive film decreases the electrostatic barrier. An increase in the substrate polarity also plays an important role by accelerating the fixation of the particles. In both cases, it is of importance that the particle concentration in the bulk droplet increases due to the evaporation of the dispersion medium, as well as in the region of the meniscus on a hydrophilic substrate, where the concentration grows owing to the transfer of the particles by the compensatory flows that arise as a result of meniscus fixation caused at an initial stage by the hysteresis of the contact angle. The growth of the concentration increases the adsorption of the particles on the substrate and the total probability of overcoming the potential barrier and adhesion to the substrate. The particles appear to be strongly bonded to the substrate and are not displaced by the forces that arise upon the displacement of the meniscus.

## ACKNOWLEDGMENTS

This work was supported by the Russian Foundation for Basic Research (projects nos. 16-08-00554a and 15-03-02300) and the Program for Basic Research of the Presidium of the Russian Academy of Sciences no. 39.

## REFERENCES

1. Molchanov, S.P., Roldughin, V.I., and Chernova-Kharaeva, I.A., *Colloid J.*, 2015, vol. 77, p. 761.
2. Molchanov, S.P., Roldughin, V.I., and Chernova-Kharaeva, I.A., *Colloid J.*, 2015, vol. 77, p. 770.
3. Molchanov, S.P., Roldughin, V.I., Chernova-Kharaeva, I.A., and Yurasik, G.A., *Colloid J.*, 2016, vol. 78, p. 633.
4. Deegan, R.D., Bakajin, O., Dupont, T.F., Huber, G., Nagel, S.R., and Witten, T.A., *Nature* (London), 1997, vol. 389, p. 827.
5. Deegan, R.D., Bakajin, O., Dupont, T.F., Huber, G., Nagel, S.R., and Witten, T.A., *Phys. Rev. E: Stat. Phys., Plasmas, Fluids, Relat. Interdiscip. Top.*, 2000, vol. 62, p. 756.

6. Kumnorkaew, P., Ee, Y.-K., Tansu, N., and Gilchrist, J.F., *Langmuir*, 2008, vol. 24, p. 12150.
7. Zhang, D., Vangala, K., Jiang, D., Zou, S., and Pechan, T., *Appl. Spectrosc.*, 2010, vol. 64, p. 1078.
8. Bhardwaj, R., Fang, X., Somasundaran, P., and Attinger, D., *Langmuir*, 2010, vol. 26, p. 7833.
9. Dugyala, V.R. and Basavaraj, M.G., *Langmuir*, 2014, vol. 30, p. 8680.
10. Yunker, P.J., Still, T., Lohr, M.A., and Yodh, A.G., *Nature* (London), 2011, vol. 476, p. 308.
11. Shen, X., Ho, C.-M., and Wong, T.-S., *J. Phys. Chem. B*, 2010, vol. 114, p. 5269.
12. Li, Y.-F., Sheng, Y.-J., and Tsao, H.-K., *Langmuir*, 2013, vol. 29, p. 7802.
13. Vysotskii, V.V., Roldughin, V.I., Uryupina, O.Ya., and Zaitseva, A.V., *Colloid J.*, 2011, vol. 73, p. 176.
14. Vysotskii, V.V., Uryupina, O.Ya., Senchikhin, I.N., and Roldughin, V.I., *Colloid J.*, 2013, vol. 75, p. 142.
15. Vysotskii, V.V., Uryupina, O.Ya., Senchikhin, I.N., and Roldughin, V.I., *Colloid J.*, 2013, vol. 75, p. 634.
16. Vysotskii, V.V., Roldughin, V.I., Uryupina, O.Ya., Senchikhin, I.N., and Zaitseva, A.V., *Colloid J.*, 2014, vol. 76, p. 531.
17. Nazarov, V.G. and Stolyarov, V.P., *Colloid J.*, 2016, vol. 78, p. 75.
18. Huang, W., Cui, L., Li, J., Luo, C., Zhang, J., Luan, S., Ding, Y., and Han, Y., *Colloid Polym. Sci.*, 2006, vol. 284, p. 366.
19. Sefiane, K. and Bennacer, R., *J. Fluid Mech.*, 2011, vol. 667, p. 260.
20. David, S., Sefiane, K., and Tadriss, L., *Colloids Surf. A*, 2007, vol. 298, p. 108.
21. Vysotskii, V.V., Roldughin, V.I., Uryupina, O.Ya., Senchikhin, I.N., and Zaitseva, A.V., *Colloid J.*, 2015, vol. 77, p. 431.
22. Roldughin, V.I., *Usp. Khim.*, 2004, vol. 73, p. 123.
23. Terekhin, V.V., Dement'eva, O.V., and Rudoy, V.M., *Usp. Khim.*, 2011, vol. 80, p. 477.
24. Lebedev-Stepanov, P.V., Kadushnikov, R.M., Molchanov, S.P., Ivanov, A.A., Mitrokhin, V.P., Vlasov, K.O., Rubin, N.I., Yurasik, G.A., Nazarov, V.G., and Alifimov, M.V., *Nanotechnol. Russ.*, 2013, vol. 8, nos. 3–4, p. 137.
25. Vysotskii, V.V., Roldughin, V.I., and Uryupina, O.Ya., *Colloid J.*, 2004, vol. 66, p. 777.
26. Bhardwaj, R., Fang, X., and Attinger, D., *New J. Phys.*, 2009, vol. 11, p. 075020.
27. Roldughin, V.I., *Fizikokhimiya poverkhnosti* (Surface Physical Chemistry), Dolgoprudnyi: Izd. Dom Intel'ekt, 2011.
28. Men'shikova, A.Yu., Shabsel's, B.M., Evseeva, T.G., Shevchenko, N.N., and Bilibin, A.Yu., *Russ. J. Appl. Chem.*, 2005, vol. 78, p. 159.
29. Stöber, W., Fink, A., and Bohn, E., *J. Colloid Interface Sci.*, 1968, vol. 26, p. 62.
30. Derjaguin, B.V. and Churaev, N.V., *Smachivayushchie plenki* (Wetting Films), Moscow: Nauka, 1984.

Translated by A. Kirilin